Rich stochastic dynamics of co-doped Er:Yb fluorescence upconversion nanoparticles in the presence of thermal, non-conservative, harmonic and optical forces

2017 Methods Appl. Fluoresc. 5 014005

(http://iopscience.iop.org/2050-6120/5/1/014005)

Methods and Applications in Fluorescence

RECEIVED
31 October 2016

REVISED
21 December 2016

ACCEPTED FOR PUBLICATION
11 January 2017

PUBLISHED
10 February 2017

PAPER

Rich stochastic dynamics of co-doped Er:Yb fluorescence upconversion nanoparticles in the presence of thermal, non-conservative, harmonic and optical forces

Rene A Nome[1], Cecilia Sorbello[2,3], Matías Jobbágy[2,3], Beatriz C Barja[2,3], Vitor Sanches[1], Joyce S Cruz[1] and Vinicius F Aguiar[1]

[1] Institute of Chemistry, University of Campinas, Campinas, SP, Brazil
[2] DQIAQF, Facultad de Ciencias Exactas y Naturales, Universidad de Buenos Aires, Pabellón II, Ciudad Universitaria, C1428EHA-Buenos Aires, Argentina
[3] INQUIMAE, CONICET, Argentina

E-mail: nome@iqm.unicamp.br

Keywords: stochastic dynamics, upconversion nanoparticles, microscopy

Supplementary material for this article is available online

Abstract

The stochastic dynamics of individual co-doped Er:Yb upconversion nanoparticles (UCNP) were investigated from experiments and simulations. The UCNP were characterized by high-resolution scanning electron microscopy, dynamic light scattering, and zeta potential measurements. Single UCNP measurements were performed by fluorescence upconversion micro-spectroscopy and optical trapping. The mean-square displacement (MSD) from single UCNP exhibited a time-dependent diffusion coefficient which was compared with Brownian dynamics simulations of a viscoelastic model of harmonically bound spheres. Experimental time-dependent two-dimensional trajectories of individual UCNP revealed correlated two-dimensional nanoparticle motion. The measurements were compared with stochastic trajectories calculated in the presence of a non-conservative rotational force field. Overall, the complex interplay of UCNP adhesion, thermal fluctuations and optical forces led to a rich stochastic behavior of these nanoparticles.

Introduction

The random Brownian motion of a small particle in solution suggests, at first glance, that its dynamics are unpredictable and, thus, that it is useless to try to obtain information about individual trajectories in viscous fluids. This is indeed the case for free diffusion driven by white noise, where the particle loses memory of its position and momentum after every collision. However, in real biological, chemical, and physical systems, it turns out that the molecular properties of the surrounding environment end up affecting particle motion and thus leading to memory effects [1, 2]. Usually, such effects are described by modifying the underlying Langevin equation [3]. Specifically, one usually incorporates a frequency-dependent friction force exerted by the environment on the particle, giving rise to so-called colored noise and time-dependent diffusion. The role of solvent friction has been extensively investigated in both molecular [4–6], biological [7, 8], and soft matter [9]. Moreover, external forces comparable to thermal forces can be included, thereby adding experimental parameters that further enrich stochastic dynamics far from equilibrium. For example, optical trapping has long been used to accelerate and bind particles with laser light and study basic thermodynamic [10, 11] and chemical and hydrodynamic [12, 13] processes in the presence of optical forces.

Despite the enormous experimental and theoretical improvements in our understanding of stochastic dynamics far from equilibrium, most studies focus on one aspect of the underlying generalized Langevin equation. Given the fascinating variety of phenomena explored in this field so far, it is interesting to think about individual particle trajectories in the presence of multiple external forces and colored noise. In the present work, we report our experimental and computational

stochastic dynamics study of gadolinium oxide nanoparticles doped with Er3+ and Yb3+ ions [14, 15]. Our experiments are performed with a home-built fluorescence upconversion micro-spectrometer that enables single-particle tracking of the upconversion nanoparticles (UCNP). Tracking these up-converting nanoparticles via IR excitation light is more convenient than via UV or visible excitation, since background emission capable of absorbing in the UV–vis range (algae, bacteria, biomolecules, tissue) is discarded and the signal to noise ratio is dramatically enhanced. By combining optical forces, thermal forces, and UCNP/surface interactions, several factors affect the measured trajectories. We perform Brownian dynamics simulations of harmonically bound spheres in the presence of non-conservative rotational forces to assess the rich stochastic behavior observed experimentally.

Material and methods

Synthesis and characterization of the samples

Phosphors' precursors were prepared by the urea method by aging several solutions containing cerium (III) nitrate hexahydrate, gadolinium(III) nitrate hexahydrate, erbium(III) nitrate pentahydrate and ytterbium(III) nitrate pentahydrate with a total cation content of (1.5×10^{-2} mol dm^{-3}) and urea (0.5 mol dm^{-3}). The ratios for each RE(III) to ([Ce(III)] + [Gd (III)] + [Er(III)] + [Yb(III)]), expressed as $\%RE$, were as described previously [14]. Typically, 50 ml of each solution were filtered, bubbled with nitrogen and aged at 363 K for 3 h. After quenching the reaction in an ice bath, the solids were filtered (0.2 μm membranes), washed with water and dried at room temperature overnight. Mixed oxides (phosphors) were synthesized by heating the precursors for 6 h at 1273 K under an air atmosphere at a 5 K min^{-1} rate. All synthesized precursors and the resulting oxides were characterized by powder x-ray diffraction (PXRD) using the graphite-filtered CuK_α radiation ($\lambda = 1.5406$ Å), with a step size of 0.02 and 2 s step time. The cell parameters were estimated from the main reflections recorded between $20 < 2\ theta < 100$. HRSEM coupled with EDS was performed on samples deposited straight onto conductive silicon wafer substrates without further metallization. HRSEM-assisted inspection of the samples revealed a common textural evolution during the annealing, irrespective of composition. Initially, the precursors consisted of spheres with smooth surfaces, typical of quasi-amorphous basic carbonates. After annealing, the aforementioned particles evolved into polycrystalline densified spheroids, exhibiting well defined crystallites approximately 180 nm size, as evidenced by the faceted surface of the oxidic particles. While the inner nanocrystallites strongly coalesced after annealing, no massive sintering was developed, allowing a significant preservation of both shape and size of the parent particles. Particle size and zeta potential measurements were performed with a 3 mg mL^{-1} aqueous suspension of the synthesized UCNP on a Zeta Sizer Nano (ZS-Zen 3600) from Malvern. Suspensions were sonicated before each measurement.

Optical trapping and microscopy

As shown in figure 2(A), the home-built optical setup consists of a 975 nm diode laser followed by a beam expander, a low-pass dichroic mirror, an inverted optical microscope with a 100x, NA = 1.30 objective (Olympus), and thus an estimated spot size of ~375 nm. Transmitted white light was detected with a CCD (Thorlabs); epi-fluorescence was detected with a spectrometer (OceanOptics) and CCD. The optical setup was placed on an optical table.

Polystyrene (PS) nanospheres with an average size of 804 ± 5 nm from Aldrich Chem. Co. were used as received. The sample was diluted by a factor of 180 000x for the single-particle optical microscopy and dynamic light scattering (DLS) measurements. The suspensions were sonicated before each measurement. The sample volume for the optical microscopy measurements was limited to 50 μl with an adhesive tape to help minimize flow due to solvent evaporation.

Quantitative digital video microscopy and Brownian motion characterization

We have used the *ImageJ* MTrack2 plugin to quantify single-particle trajectories from the recorded optical microscopy image sequences. We perform pixel-by-pixel background noise subtraction by recording the same region without the particle during the same period of time. The trajectory analysis gives a table indicating the image frame and the particle position (x and y). Free diffusion characterization was performed by analyzing trajectories of PS nanoparticles suspended in water. It is important to remark that the free diffusion studies were performed with transmitted light and the excitation/trapping laser blocked. We have employed three diffusion coefficient determination methods: both (i) histogram analysis and (ii) mean-square displacement (MSD) analysis, and (iii) power-spectrum density-based diffusion coefficient determination as described in [16]. The results of these control experiments and associated analysis are shown in the supporting information.

Simulations

We solve the Langevin equation of motion using [17]:

$$\gamma \frac{\mathrm{d}x}{\mathrm{d}t} = -\frac{1}{m}\frac{\mathrm{d}V(x)}{\mathrm{d}x} + \frac{1}{m}\delta F(t),$$

where γ is the friction coefficient, m is the particle mass, $V(x)$ is the potential energy, $\delta F(t)$ is a random force with zero mean and variance:

$$\langle \delta F(t)\delta F(t')\rangle = 2\gamma k_B T \delta(t - t').$$

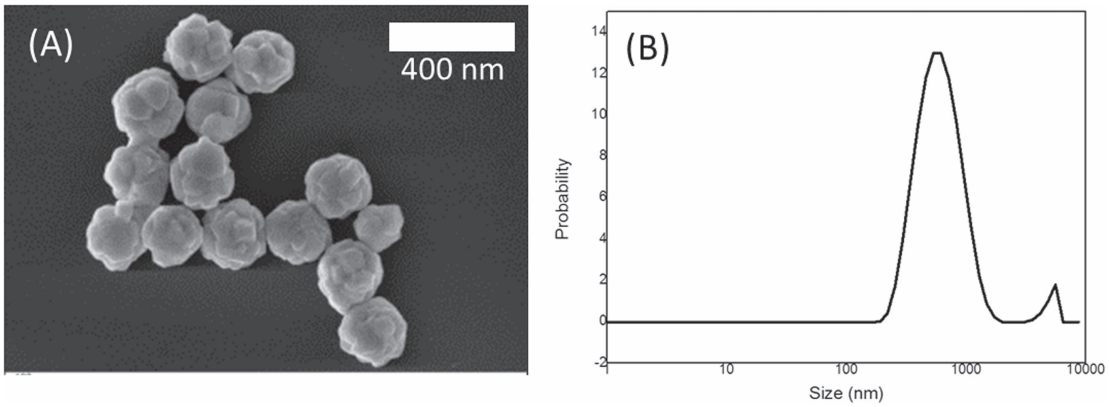

Figure 1. UCNP characterization. (A) HRSEM images. (B) Size distribution as measured by dynamic light scattering from a 3 mg ml^{-1} suspension of UCNP in water.

Results and discussion

HRSEM revealed polycrystalline multifaceted particles with an average size of 180 nm and a spheroidal shape, consistent with our previous SEM and PXRD characterization of this sample [14]. Light scattering measurements of 3 mg ml^{-1} UCNP aqueous suspension resulted in a zeta potential of $+20 \pm 3.5$ mV (not shown) and a particle size of 606 ± 257 nm with polydispersity PdI $= 0.258$, as shown in figure 1(B). We have also observed an additional peak at 5.096 μm $\pm$ 571.3 nm with a small 3.3% contribution to the measured signal. The main contribution to the DLS size distribution plot shown in figure 1(B) indicates that the nanoparticles in solution are approximately 2–3 times larger in solution than in the solid state (figure 1(A)), presumably due to aggregation. We sought additional evidence for aggregation in the SEM images and DLS measurements. First, as suggested by the SEM images of the UCNPs shown in figure 1(A) and in [14], the polycrystalline nature of these UCNP may lead to chemical aggregation between individual facets of nearby nanoparticles, thereby resulting in aggregate formation. Second, DLS experiments performed in ethanol/water mixtures containing UCNPs resulted in a hydrodynamic size of 316 nm (see the supporting information), which is closer to the particle size observed in the SEM image shown in figure 1(A). In what follows, we focus on studies performed in aqueous solutions containing UCNPs with an overall size, as shown in figure 1(B); such particle size and zeta potential are suitable for our quantitative optical microscopy studies of stochastic dynamics under the presence of thermal, harmonic, and non-conservative forces described below.

Our setup, shown schematically in figure 2(A), allows us to measure upconversion luminescence spectra, single-photon counting, optical and dark field microscopies and optical trapping. Figure 2(B) shows the luminescence spectra of UCNP measured in solution together with the corresponding spectral assignment. The upconversion process permits the excitation in the IR region to obtain emission in the visible range (red and green) [18, 19]. This anti stokes conversion of energy is a nonlinear multiphoton process in which photons of the same low energy (IR) are absorbed by an atom and then sequentially excited to higher equally spaced metastable energy states from which light in the vis range can be emitted. Lanthanides fullfil these two conditions: their levels are sequentially spaced (Er3+) with real, (non virtual) metastable states (lifetimes in the μs–ms range). The upconversion mechanisms have been extensively studied for the pair Er3+/Yb3+ in different host matrices [20, 21]. Overall, we find good agreement between the upconversion spectra measured in solution and previously reported co-doped Er:Yb nanoparticle upconversion spectra. Spectral differences in this region are presumably due to solvent and aggregation effects as well as intensity-dependent focusing and nonlinear processes.

In the present work, our focus is on measuring and modelling the stochastic dynamics of UCNP. Thus, the results shown in figure 2(B) are of interest because of the high upconversion luminescence intensity that ensured data acquisition with a high signal-to-noise ratio and moderate accumulation times. For example, figure 2(C) shows UCNP integrated emission intensity as a function of time for a period of approximately 10 s. The signal modulation shown in figure 2(C) is associated with turning the laser ON and OFF. At 300 mW laser power, single-particle upconversion luminescence signals were observed at high count-rates (approximately 175 kcounts/s). Figure 2(D) shows a fluorescence upconversion microscopy image from a single UCNP indicating high spatial resolution and nanoparticle localization. The inset of figure 2(D) shows our optical trapping calibration curve obtained from the equipartition theorem for the measured position distribution histogram for a polystyrene particle subjected to thermal fluctuations and a harmonic potential well created at the laser focus [13]. The

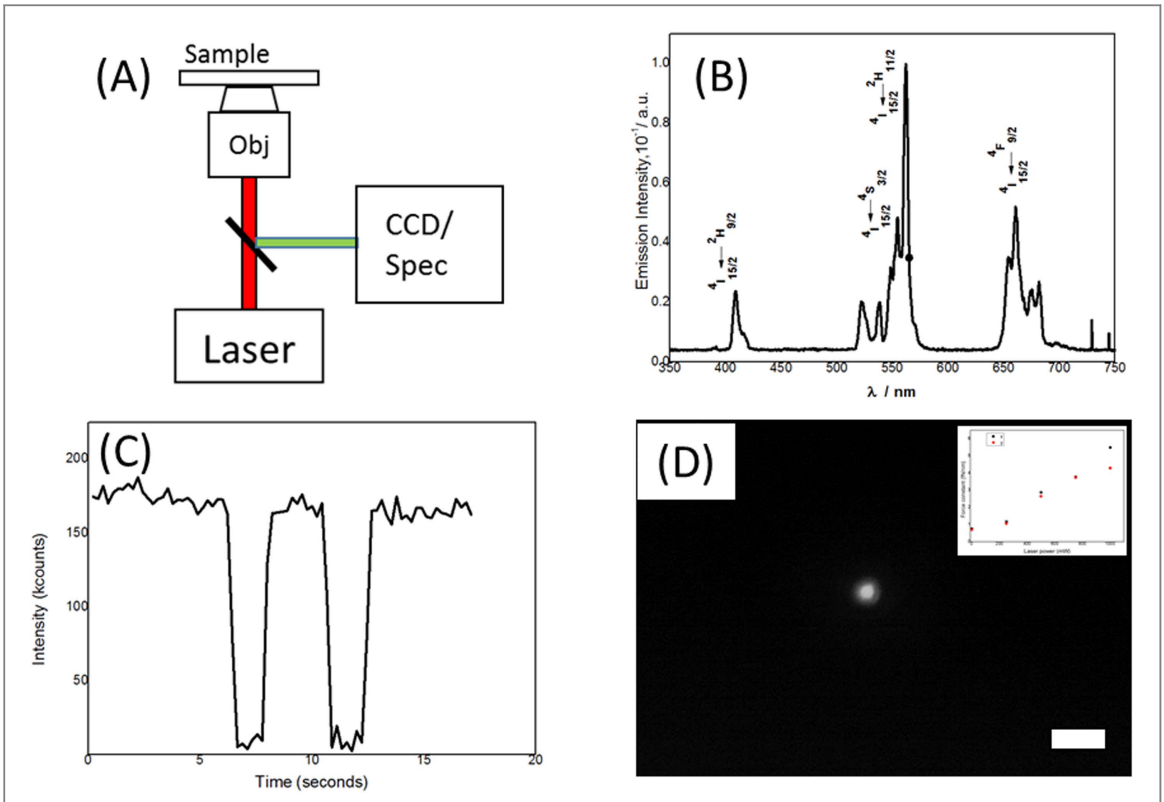

Figure 2. Optical and fluorescence upconversion microscopy and spectroscopy of UCNP. (A) Schematic description of the setup used in the present work. (B) Fluorescence upconversion spectrum of UCNP in water. Peak assignments are indicated in the spectrum. (C) Fluorescence upconversion time series for a single UCNP. A sudden decrease/increase in intensity corresponds to the instant at which the laser was respectively turned OFF/ON. (D) Fluorescence upconversion microscopy of a single UCNP. Scale bar represents 1 μm. Inset: optical trapping force constant calibration curve. The experimental data shown (B), (C), and (D) correspond to fluorescence upconversion from a single UCNP placed at the excitation/optical trapping laser beam focus. All experiments were performed with laser power = 300 mW.

trapping force constant increases from 1 to 6 fN nm^{-1} as the laser power is increased from 250 mW to 1 W. The results demonstrate a linear behavior for the force constant as a function of output laser power in the 250–750 mW range, which is compatible with results from the literature [22]. At a higher laser power, there is a difference with respect to ideal behavior, since in theory the laser beam produces a symmetric potential in the x and y directions, which is not observed in the results obtained at 1 W. This discrepancy may be due to water IR absorption and/or artifacts in particle position determination. In the present work, we have studied optical forces on UCNP at 300 mW laser power, which is within the linear working range of our optical trapping apparatus.

Employing the sample and methods described above, we have observed rich stochastic dynamics behavior of UCNP subjected to thermal and non-thermal forces. First, we have observed the adhesion of UCNP to the microscope slide, presumably due to electrostatic interaction between the microscope slide and the positively charged nanoparticle surface (zeta potential = +20 mV). Figure 3(A) is a log–log plot of the MSD as a function of time for UCNP on the slide surface. The MSD increases at short times and approaches a saturation value at longer timescales. We exclude the possibility of observing an inertial-to-diffusive regime due to the nanoparticle short momentum relaxation time, which slows further near the surface [23, 24]. Rather, the plot shown in figure 3(A) indicates that the UCNP can diffuse near the surface for short periods of time but are unable to move away from the surface at longer timescales. These two regimes suggest that nanoparticle adhesion to the surface is weak compared to thermal fluctuations.

We model our measured time-dependent diffusion coefficient by numerically solving the Langevin equation for a harmonically bound 1 μm diameter sphere immersed in water at 298 K [9]. Figure 3(B) shows a log–log plot of MSD as a function of time obtained numerically for a harmonic spring constant ranging from 0.1 fN nm^{-1}–5 fN nm^{-1}. At all times, the calculated MSD exhibits time-dependence which is qualitatively similar to the one shown in figure 3(A) [25, 26]. In the limit of weakly bound spheres, the MSD is diffusive at nearly all timescales, although it still reaches a plateau at longer times. On the other hand, the particles exhibit a MSD saturation at shorter times as the spring constant increases, thus being unable to move away at longer times. Despite the similarity between measured and calculated MSD, we have not obtained a satisfactory fit using this time-dependent diffusion model. Nonetheless, given that the

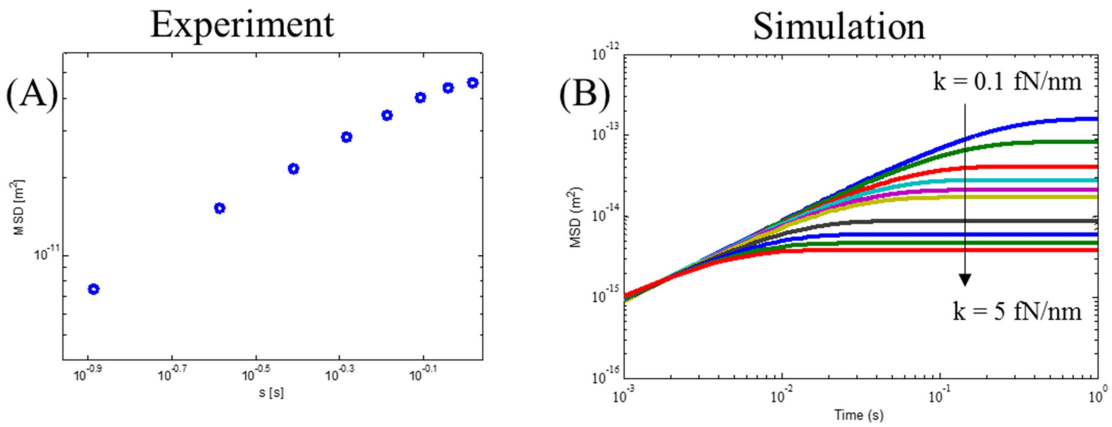

Figure 3. Stochastic dynamics of individual UCNP from experiment and simulation. (A) Mean-squared displacement (MSD) as a function of time calculated from an individual UCNP trajectory measured with the setup shown in figure 2. (B) MSD as a function of time calculated from Brownian dynamics simulations of harmonically bound spheres.

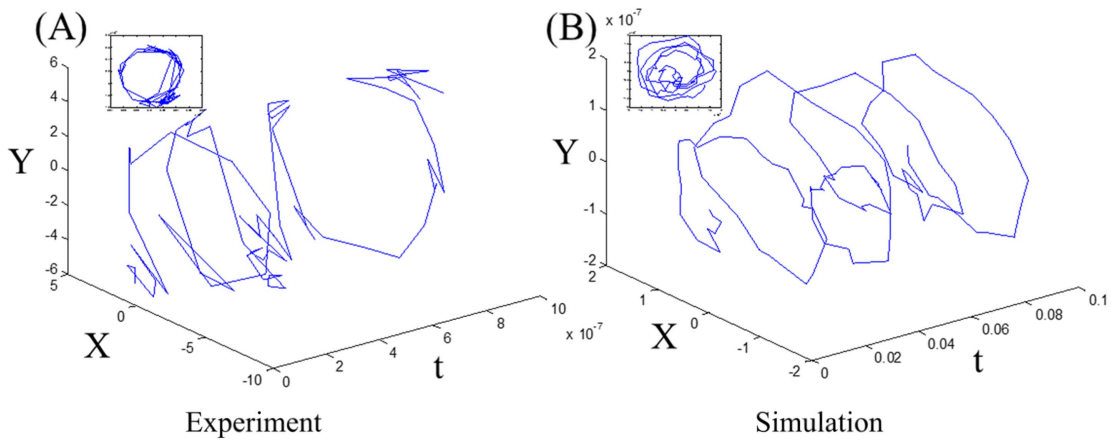

Figure 4. Stochastic dynamics of individual UCNP from experiment and simulation. (A) Experimental time-dependent two-dimensional trajectory of an individual UCNP. Inset: experimental trajectory projected on to the *XY* plane. (B) Calculated time-dependent two-dimensional trajectory from Brownian dynamics simulations of harmonically bound spheres in the presence of a non-conservative rotational force field. Inset: calculated trajectory projected onto the *XY* plane. In both (A) and (B), *X* and *Y* are positions in μm and *t* is time in seconds.

same qualitative trends are observed for the time-dependent MSD in both experiment and simulations, we believe this viscoelastic model is a useful starting point for understanding the stochastic dynamics of UCNP near the surface.

To further investigate the dynamics of UCNP near the surface, we analyze the time-dependent two-dimensional nanoparticle trajectories obtained experimentally. Figure 4(A) is a plot of the nanoparticle center position in the *XY* plane as a function of time. Although the trajectory is complex, one can observe that the nanoparticle performs two clockwise rotations during the first 3 s of measurement. To see such circular motion more clearly, the inset of figure 4(A) shows the complete experimentally measured trajectory projected onto the *XY* plane. To a first approximation, the nanoparticle trajectory can be reasonably described by a circle with a diameter of 0.9 μm, which is 50% larger than the nanoparticle size. Furthermore, at time t $\sim$ 4 s, the nanoparticle motion shifts by 180 degrees and the trajectory performs (nearly) two additional counter-clockwise rotations.

We introduce a non-conservative rotational force field term to our model to describe the trajectory shown in figure 4(A). The force term to be introduced in the two-dimensional Langevin equation is [27]:

$$\vec{F}(x, y) = -\begin{bmatrix} k & \gamma\Omega \\ -\gamma\Omega & k \end{bmatrix}\begin{bmatrix} x \\ y \end{bmatrix}$$

where Ω is the rotational frequency. Figure 4(B) is the particle trajectory obtained numerically from Langevin dynamics simulations of the augmented viscoelastic model, including rotational force. We have used the same simulation parameters as before, plus a rotational frequency. As in the experimental result, the trajectory is stochastic and complex. However, we obtain a similar-looking *x*–*y* correlated motion in the simulations as in the experiment, with clockwise rotations of the particle trajectory as a function of time. Furthermore, by introducing a 180° phase shift to the rotational

force field given above, we also observe counter-clockwise particle trajectory rotation in the simulations.

Conclusions

We have performed experimental and computational stochastic dynamics studies of individual co-doped Er:Yb UCNP. The UCNP were characterized by electron and optical microscopy, light scattering and fluorescence upconversion. We have performed single-particle optical microscopy studies of UCNP with a home-built apparatus employing a 980 nm diode laser for optical trapping and upconversion excitation. We have performed single-particle measurements of UCNP. MSDs from single UCNP exhibited a time-dependent diffusion coefficient which were compared with Brownian dynamics simulations of a viscoelastic model of harmonically bound spheres. Experimental time-dependent two-dimensional trajectories of individual UCNP revealed correlated two-dimensional nanoparticle motion. The measurements were compared with stochastic trajectories calculated in the presence of a non-conservative rotational force field. Overall, the complex interplay of UCNP adhesion, thermal fluctuations and optical forces led to a rich stochastic behavior of these nanoparticles.

Acknowledgments

Financial support from CNPq, CAPES, is gratefully acknowledged. We thank Bruno Zornio for his assistance with the PS free diffusion measurements.

References

[1] Bialek W 2012 *Biophysics: Searching for Principles* (Princeton: Princeton University Press)
[2] Nitzan A 2006 *Chemical Dynamics in Condensed Phases* (New York: Oxford University Press)
[3] Zwanzig R W 2001 *Nonequilibrium Statistical Mechanics* (New York: Oxford University Press)
[4] Anna J M and Kubarych K J 2010 Watching solvent friction impede ultrafast barrier crossing: a direct test of Kramers Theory *J. Chem. Phys.* **133** 174506
[5] Fleming G R, Courtney S H and Balk M W 1986 Activated barrier crossing: comparison between experiment and theory *J. Stat. Phys.* **42** 83–104
[6] Rothenberger G, Negus D K and Hochstrasser R M 1983 *J. Chem. Phys.* **79** 53–60
[7] Grote R F and Hynes J T 1980 *J. Chem. Phys.* **73** 215–20
[8] Silva R G, Murkin A S and Schramm V L 2011 Femtosecond dynamics coupled to barrier crossing in a Born–Oppenheimer enzyme *PNAS* **108** 18661–5
[9] Mason T G and Weitz D A 1995 Optical measurements of frequency-dependent linear viscoelastic moduli of complex fluids *Phys. Rev. Lett.* **74** 1250–3
[10] Ashkin A 1970 Acceleration and trapping of particles by radiation pressure *Phys. Rev. Lett.* **24** 156–9
[11] Crocker J C, Matteo J A, Dinsmore A D and Yodh A G 1999 Entropic attraction and repulsion in binary colloids probed with a line optical tweezer *Phys. Rev. Lett.* **82** 4352–5
[12] Chen F-J *et al* 2012 Thermally activated state transition technique for femto-Newton-level force measurement *Opt. Lett.* **37** 1469–71
[13] Phillips D B 2011 Optimizing the optical trapping stiffness of holographically trapped microrods using high-speed video tracking *J. Opt.* **13** 044023
[14] Sorbello C, Barja B C and Jobbagy M 2014 Monodispersed Ce(IV)-Gd(III)-Eu(III) oxide phosphors for enhanced red emission under visible excitation *J. Mater. Chem.* C **2** 1010–7
[15] Di Leonardo R, Cammarota E, Bolognesi G, Schafer H and Steinhart M 2011 Three-dimensional to two-dimensional crossover in the hydrodynamic interactions between micron-scale rods *Phys. Rev. Lett.* **107** 044501
[16] Vestergaard C L, Blainey P C and Flyvbjerg H 2014 Optimal estimation of diffusion coefficients from single-particle trajectories *Phys. Rev.* E **89** 022726
[17] Langevin P 1908 Sur la théorie du mouvement brownien *CR Acad. Sci. (Paris)* **146** 530–3
[18] Auzel F 2004 Upconversion and Anti-Stokes processes with f and d ions in solids *Chem. Rev.* **104** 139–73
[19] Liu X, Yan C-H and John A C 2015 *Chem. Soc. Rev.* **44** 1299–301 (Volume dedicated to photon upconversion nanomaterials)
[20] Rodrigues E M, Mazali I O and Sigoli F A 2013 Luminescent properties of passivated europium(III)-doped rare earth oxide sub-10 nm nanoparticles *RSC Adv.* **3** 2794–801
[21] Schafer H and Haase M 2011 Upconverting nanoparticles *Angew. Chem., Int. Ed. Engl.* **50** 5808–29
[22] Singer W *et al* 2000 Three-dimensional force calibration of optical tweezers *J. Mod. Opt.* **47** 2921–31
[23] Li T *et al* 2010 Measurement of the instantaneous velocity of a Brownian particle *Science* **328** 1673–5
[24] Huang R *et al* 2011 Direct observation of the full transition from ballistic to diffusive Brownian motion in a liquid *Nat. Phys.* **7** 576–80
[25] Qian H, Sheetz M P and Elson E L 1991 Single particle tracking. Analysis of diffusion and flow in two-dimensional systems *Biophys. J.* **60** 910–21
[26] Saxton M J 1997 Single-particle tracking: the distribution of diffusion coefficients *Biophys. J.* **72** 1744–53
[27] Volpe G and Volpe G 2013 Simulation of a Brownian particle in an optical trap *Am. J. Phys.* **81** 224